Journal of Solid Mechanics Vol. 12, No. 1 (2020) pp. 219-233
DOI: 10.22034/jsm.2019.1869652.1447

Clamped-Free Non Homogeneous Magneto Electro Elastic Plate of Polygonal Cross-Sections with Hydrostatic Stress and Gravity

G. Infant Sujitha [1], R. Selvamani [2,*]

[1]*Department of Science and Humanities, Sri Krishna College of Engineering and Technology, Coimbatore-641008, Tamil Nadu, India*
[2]*Department of Mathematics, Karunya University, Coimbatore-641114, Tamil Nadu, India*

Received 3 January 2020; accepted 2 March 2020

ABSTRACT

In this article, the influence of hydrostatic stress and gravity on a clamped- free non-homogeneous magneto electro elastic plate of polygonal cross sections is studied using linear theory of elasticity. The equations of motion based on two-dimensional theory of elasticity are applied under the plane strain assumption of pre-stressed and gravitated magneto electro elastic plate of polygonal cross-sections composed of non-homogeneous isotropic material. The frequency equations are obtained by satisfying the boundary conditions along the irregular surface of the polygonal plate using Fourier expansion collocation method. The complex roots of the frequency equations are obtained by secant method. The numerical computations are carried out for triangular, square, pentagon and hexagon cross sectional plates. Graphical representation is given for the various physical variables via gravity and different edge boundaries and its characteristics are discussed. This result can be applied for optimum design of concrete plates with polygonal cross sections.

Keywords: Stress-strain relation; Non-homogeneous; Pre-stressed and gravitated poly plate; FECM.

1 INTRODUCTION

THE hydrostatic concrete solid plates are used in the construction to increase the inner tensile strength. It is widely used in the reduction of structural thickness with the improvement for longer span. The pre-stressed floor slabs consists of bracing wire strings, steel bars are laid over the reinforcement, which are having the longitudinal property. The most advantage of these types of floor slabs is large available span with minimal amount of support. These floor slabs are used in the structural engineering such as multi story car parking, residential, super market etc. Akbar [1] discussed various physical properties of multi layered, mechanical loaded cylinders. Mohammad Arefi et al. [2] presented the thermo elastic analysis of FG cylinder subjected to axially variable thermal and mechanical loads. Khoshgoftar et al. [3] used shear deformation theory to derive the analytical solution of functionally graded

*Corresponding author.
E-mail address: selvam1729@gmail.com (R. Selvamani).

cylinder with finite length thick cylinder under non-uniform pressure. Mohammed Arefi and Rahimi [4] discussed the thermo elastic behavior of clamped-clamped functionally graded cylinder under internal pressure also calculated the SCF due to clamping. Later, Mohammad Arefi [5] carried out the analytical investigation on the nonlinear behavior of the functionally graded piezoelectric cylinder along the thickness direction. He gave the nonlinear result, which justifies the importance of nonlinear analysis used in the sensors and actuator. Abbas et al. [6] used complex Fourier series to analyze the non-symmetric thermo elasticity of functionally graded cylinder and obtained the result that the considerable effect of loading on the non-symmetric behavior of the FG cylinder. Rahimi [7] introduced the term additional energy to the exact energy functional of a functionally graded piezo electrical rotating cylinder and obtained that the electrical potential is proportional to angular velocity. Nagaya [8, 11] derived a method for finding the solution of vibration problems on an arbitrary cross sectional plate. He also discussed the dispersion of the elastic waves in the cylindrical bars with the polygonal cross sections. Hutchinson [9] discussed the axisymmetric flexural waves over a thick circular plate. The effect of non-homogeneity and boundary conditions of a functionally graded circular plate on the Winkler-Pasternak foundation were investigated by Mohammed Arefi and Allam [10,12].Also he presented the nonlinear analysis of functionally graded square plate with piezoelectric layers resting on the Winkler-Pasternak foundation and gave the comparison between linear and nonlinear responses of the considered system. Chakraverty et al. [13] studied the flexural vibrations of non-homogeneous elliptic plates. Tanigawa [14] presented some basic thermoelastic problems for non-homogeneous structural materials. Annibale et al.[15] derived the stability of the discrete mechanical system which is controllable by the peizo electric nature. Selvamani [16] analyzed the elasto dynamic wave propagation in a piezo electric plate which is having the effect of fluid. Bin et al. [17] analyzed the wave propagation in non-homogeneous magneto-electro-elastic plates. Chen et al. [18] worked on free vibration of non-homogeneous transversely isotropic magneto-electro-elastic plate. Li [19] discussed the magneto electro elastic multi-inclusion and inhomogeneity problems and their applications in composite materials. Kong et al.[20] presented the thermo-magneto-dynamic stresses and perturbation of magnetic field vector in a non-homogeneous hollow cylinder. Rajneesh [21] discussed various behavior of the porous magneto electro elastic medium. Pan[22] and Pan and Heyliger [23] analyzed the three-dimensional behavior of magneto electro elastic laminates under simple support boundary conditions. Pan and Han [24] studied the exact solution for functionally graded and layered magneto-electro-elastic plates. Feng and Pan[25] discussed the dynamic fracture behavior of an internal interfacial crack between two dissimilar magneto-electro-elastic plate. Rajneesh [26] solved the wave propagation in a slightly stretched elastic solid material. Selim [27] discussed the dissipation of the torsional wave in a prestressed cylinder. Rajneesh [28] studied the problem of propagation of wave and the reflection of plane waves under the initial stress on the generalized transversely isotropic half space which is insulated thermally. Akbarov [29] presented the numerical results on the influence of the initial compression on the three layered hollow cylinders along the direction of torsional wave propagation. Kakar[30] discussed the magneto elastic torsional surface waves in the prestressed fiber reinforced medium. Wave propagation in compressed materials with reinforcement in preferred direction subjected to gravity and initial compression reads from Kakar [31]. Kumari [32] investigated the edge wave propagation on the visco elastic initially stressed plate. Wilson[36] investigated the propagation of elastic waves with strain energy in a pre stressed plate and also derived the dispersion equation. De [33] modified the classical equations of motion using Biot's theory for the elastic wave propagation in a homogeneous isotropic elastic solid medium with the assumption that the gravitational force creates an initial stress naturally. Dey [34] used the damped equation in the complex form for the effect of torsional waves in a prestressed cylinder. Chen [35] discussed the exact solution of waves in the pre stretched electro active cylinders. Zhang[37] discussed the effects of initial stress on the frequency variables and solved the guided wave propagation under gravity in the single directed plate. Lofty [38] solved the effect of the gravity and analyzed the energy dissipation of fiber reinforced thermo elastic. He analyzed also the magnetic effect on the considered material. He represented the graph with the damping and the initial stress. Ahamed [39] analyzed and gave the determinant form of equation the impact of the gravity on wave propagation in a granular medium. Hou [40] used the general solutions of transversely isotopic electro magneto thermo elastic material and constructed the three dimensional Green's function for a steady point heat source in the semi infinite transversely isotopic electro magneto thermo elastic material.

We have formulated the problem on the non-homogeneous wave propagation in a prestressed magneto piezoelectric polygonal plate. The plate possesses the gravitational force and the plate is kept in the magnetic field. The solution of the problem is derived using the Bessel function by considering the convenient form to uncouple the terms. The double Fourier series and the collocation methods are used to obtain the frequency equations for the polygonal shape of the plate. The numerical results and graphical representations are presented for the impact of different edge conditions and the gravitational force on physical variables.

2 FORMULATION OF THE PROBLEM

The considered non homogeneous hydro static magneto electro poly plate is having the stress displacement and the constitutive stress-strain relations for linear elastic medium in polar cylindrical coordinates (r,θ,t) in the absence of body force from Kakar [30] as follows:

$$\Pi_{rr,r}+r^{-1}\Pi_{r\theta,\theta}+r^{-1}\left(\Pi_{rr}-\Pi_{\theta\theta}\right)-p_s\left[u_{r,rr}+\frac{u_{r,r}}{r}-\frac{u_r}{r^2}+\frac{u_{r,\theta\theta}}{r^2}\right]+\rho g v_r=\rho u_{r,tt} \tag{1}$$

$$\Pi_{r\theta,r}+r^{-1}\Pi_{\theta\theta,\theta}+2r^{-1}\Pi_{r\theta}-p_s\left[u_{\theta,rr}+\frac{u_{\theta,r}}{r}-\frac{u_\theta}{r^2}+\frac{u_{\theta,\theta\theta}}{r^2}\right]-\rho g v_\theta=\rho u_{\theta,tt} \tag{2}$$

where $\Pi_{rr},\Pi_{r\theta},\Pi_{\theta\theta}$ the stress components and ρ are is the mass density of the material, p_s denotes the prestressed factor(when $P_s<0$ is hydrostatic tension and $P_s>0$ represents hydrostatic compression) and g is the gravitational force. u_r,u_θ are the displacement components.

The electric conduction equation is given by [41],

$$\mathbb{C}_{r,r}+r^{-1}\mathbb{C}_r+r^{-1}\mathbb{C}_{\theta,\theta}=0 \tag{3}$$

The magnetic conduction equation is given by [41],

$$\mathbb{N}_{r,r}+r^{-1}\mathbb{N}_r+r^{-1}\mathbb{N}_{\theta,\theta}=0 \tag{4}$$

where $\mathbb{C}_r,\mathbb{C}_\theta$ and $\mathbb{N}_r,\mathbb{N}_\theta$ are electric displacements and magnetic displacement components. The mechanical, electrical and magnetic stress strain relation for the isotropic material is given as:

$$\Pi_{rr}=\lambda\left(e_{rr}+e_{\theta\theta}\right)+2\mu e_{rr} \tag{5}$$

$$\Pi_{\theta\theta}=\lambda\left(e_{rr}+e_{\theta\theta}\right)+2\mu e_{\theta\theta} \tag{6}$$

$$\Pi_{r\theta}=2\mu e_{r\theta} \tag{7}$$

$$\mathbb{C}_r=\varepsilon_{11}E_r+m_{11}H_r \tag{8}$$

$$\mathbb{C}_\theta=\varepsilon_{11}E_\theta+m_{11}H \tag{9}$$

and

$$\mathbb{N}_r=m_{11}E_r+\mu_{11}H_r \tag{10}$$

$$\mathbb{N}_\theta=m_{11}E_\theta+\mu_{11}H_\theta \tag{11}$$

In which

$$E_r=-E_{,r} \text{ and } E_\theta=r^{-1}E_{,\theta} \quad H_r=-H_{,r} \quad H_\theta=r^{-1}H_{,\theta} \tag{12}$$

where λ, μ are Lame's constants, ε_{11} is the dielectric constant and m_{11}, μ_{11} are the electro-magneto material coefficients and magnetic displacements respectively. E_r, E_θ are the electric potentials, H_r, H_θ are the magnetic potentials. The strain e_{ij} can be represented by displacement as:

$$e_{rr} = u_{r,r} \tag{13}$$

$$e_{\theta\theta} = r^{-1}\left(u_r + u_{\theta,\theta}\right) \tag{14}$$

$$e_{r\theta} = u_{\theta,r} - r^{-1}\left(u_\theta - u_{r,\theta}\right) \tag{15}$$

The stress equation of motion is obtained in the following form

$$\Pi_{rr} = (\lambda + 2\mu)u_{r,r} + \lambda r^{-1}\left(u_r + u_{\theta,\theta}\right) \tag{16}$$

$$\Pi_{\theta\theta} = \lambda u_{r,r} + (\lambda + 2\mu)r^{-1}\left(u_r + u_{\theta,\theta}\right) \tag{17}$$

$$\Pi_{r\theta} = 2\mu\left(u_{\theta,r} - r^{-1}\left(u_\theta - u_{r,\theta}\right)\right) \tag{18}$$

Since the material properties vary in the direction of thickness, the material constants can be taken with the rational number 'm' and the non-homogeneous form of the equation of motion is obtained by the following substitution

$$\lambda = \lambda r^{2m}, \mu = \mu r^{2m}, m_{11} = m_{11} r^{2m}, \varepsilon_{11} = \varepsilon_{11} r^{2m}, \rho = \rho r^{2m} \tag{19}$$

Upon using the Eqs. (16)-(18) together with Eq.(19) in Eqs.(1)-(4) ,we can get the following displacement equation of motions for non-homogeneous material

$$\begin{aligned}&(\lambda + 2\mu - p_s)\left(u_{r,rr} + r^{-1}u_{r,r} - r^{-2}u_r\right) + (2\mu - p_s)r^{-2}u_{r,\theta\theta} + r^{-1}(\lambda + 2\mu)u_{\theta,r\theta} \\ &-r^{-2}(\lambda - 2m\lambda - 4\mu)u_{\theta,\theta} + 2mr^{-1}\left((\lambda + 2\mu)u_r + \lambda r^{-1}u_r\right) - \rho g v_r = \rho u_{r,tt}\end{aligned} \tag{20}$$

$$\begin{aligned}&(2\mu - p_s)\left(u_{\theta,rr} + r^{-1}u_{\theta,r} - r^{-2}u_\theta\right) + r^{-2}(\lambda + 2\mu - p_s)u_{\theta,\theta\theta} + r^{-2}(\lambda + 4m\mu + 2\mu)u_{r,\theta} \\ &+r^{-1}(4m\mu + 4\mu - p_s)u_{\theta,r} + \lambda r^{-1}u_{r,r\theta} + 2\mu r^{-1}u_{r,\theta\theta} + \rho g v_\theta = \rho u_{\theta,tt}\end{aligned} \tag{21}$$

$$\varepsilon_{11}\left(E_{,rr} + r^{-1}E_{,r} + r^{-2}E_{,\theta\theta}\right) + m_{11}\left(H_{,rr} + r^{-1}H_{,r} + r^{-2}H_{,\theta\theta}\right) + 2mr^{-1}\left(\varepsilon_{11}E_{,r} + m_{11}H_{,r}\right) = 0 \tag{22}$$

$$m_{11}\left(E_{,rr} + r^{-1}E_{,r} + r^{-2}E_{,\theta\theta}\right) + \mu_{11}\left(H_{,rr} + r^{-1}H_{,r} + r^{-2}H_{,\theta\theta}\right) + 2mr^{-1}\left(m_{11}E_{,r} + \mu_{11}H_{,r}\right) = 0 \tag{23}$$

3 SOLUTION OF THE PRESTRESSED AND GRAVITATED POLY PLATE

The recent Eqs.(20)-(23) are coupled partial differential equations and it can be uncoupled by considering the following solution of the form

$$u_r(r,\theta)=\sum_{n=0}^{\infty}\varepsilon_n\left[\left(r^{-1}\psi_{n,\theta}-\phi_{n.,r}\right)+\left(r^{-1}\overline{\psi}_{n,\theta}-\overline{\phi}_{n,r}\right)\right] \tag{24}$$

$$u_\theta(r,\theta)=\sum_{n=0}^{\infty}\varepsilon_n\left[\left(r^{-1}\phi_{n,\theta}-\psi_{n,r}\right)+\left(r^{-1}\overline{\phi}_{n,\theta}-\overline{\psi}_{n,r}\right)\right] \tag{25}$$

$$E(r,\theta)=\sum_{n=0}^{\infty}\varepsilon_n\left(E_n+\overline{E}_n\right) \tag{26}$$

$$H(r,\theta)=\sum_{n=0}^{\infty}\varepsilon_n\left(H_n+\overline{H}_n\right) \tag{27}$$

where $\varepsilon_n=1/2$ for $n=0$ and $\varepsilon_n=1$ for $n\geq 1$. By introducing the non dimensional quantity $\Omega^2=\dfrac{\rho^2\omega^2(a+b)}{2\lambda}$ where *a* and *b* are the inner and outer radius of the polygonal plate ω is the angular velocity and Substituting Eqs.(24)-(27) in Eqs.(20)-(23),we get the following decoupled equations in the following form

$$(\lambda+2\mu-p_s)\nabla^2\phi_n+mr^{-1}(2\lambda+\mu-p_s)\phi_{n,r}-2mr^{-2}\lambda\phi_n-\rho(gv_r-\phi_{n,tt})=0 \tag{28}$$

$$(2\mu-p_s)\nabla^2\psi_n+(4\mu-p_s)m\left(r^{-1}\psi_{n,r}-r^{-1}\psi_n\right)+\rho g v_\theta=0 \tag{29}$$

$$\varepsilon_{11}\nabla^2E_n+m_{11}\nabla^2H_n+2mr^{-1}\left(\varepsilon_{11}E_{n,r}+m_{11}H_{n,r}\right)=0 \tag{30}$$

$$m_{11}\nabla^2E_n+\mu_{11}r^{-2m}\nabla^2H_n+2mr^{-1}\left(m_{11}E_{n,r}+2\mu r^{-2m}H_{n,r}\right)=0 \tag{31}$$

where $\nabla^2=\dfrac{\partial^2}{\partial r^2}+\dfrac{1}{r}\dfrac{\partial}{\partial r}+\dfrac{1}{r^2}\dfrac{\partial^2}{\partial\theta^2}$.

We consider the free vibration of non-homogeneous polygonal cross-sectional plate and we seek the displacement function, electric and magnetic displacement function as:

$$\phi_n(r,\theta,t)=r^{-m}\phi_n(r)\cos n\theta e^{i\omega t} \tag{32}$$

$$\psi_n(r,\theta,t)=r^{-m}\psi_n(r)\cos n\theta e^{i\omega t}. \tag{33}$$

$$E_n(r,\theta,t)=r^{-m}E_n(r)\cos n\theta e^{i\omega t} \tag{34}$$

$$H_n(r,\theta,t)=r^{-m}H_n(r)\cos n\theta e^{i\omega t} \tag{35}$$

Using the Eqs. (32)-(33) in the Eqs. (28)-(29), we get

$$\phi_n''(r)+r^{-1}\phi_n'(r)\left(1-\frac{3m\mu+mp_s}{\lambda+2\mu-p_s}\right)+r^{-2}\phi_n(r)\left[\frac{m^2(\mu-\lambda)+2m\lambda-\rho(gv_r-\omega^2r^2)}{\lambda+2\mu-p_s}-n^2\right]=0 \tag{36}$$

$$\psi_n''(r)+r^{-1}\psi_n'(r)\left(\frac{m-1}{2\mu-p_s}\right)+r^{-2}\psi_n(r)\left[\frac{\rho(gv_\theta+m^2-1)}{2\mu-p_s}-(m^2-n^2)\right]=0 \tag{37}$$

The above equation can be reduced to the following forms of Bessel equations

$$\begin{aligned}&\phi_n^{''}(r)+r^{-1}\phi_n^{'}(r)+\phi_n(r)r^{-2}(n^2r^2-\beta^2)=0\\&\psi_n^{''}(r)+r^{-1}\psi_n^{'}(r)+r^{-2}\psi_n(r)((m^2-n^2)r^2-\delta^2)=0\end{aligned} \tag{38}$$

and the corresponding solution is obtained by

$$\begin{aligned}&\phi_n(r)=\left(P_{1n}J_\beta(Nr)+P_{1n}^{'}Y_\beta(Nr)\right)\cos n\theta\\&\psi_n(r)=\left(P_{2n}J_\delta(Mr)+P_{2n}^{'}Y_\delta(Mr)\right)\cos n\theta\end{aligned} \tag{39}$$

Here P_{1n}, $P_{1n}^{'}$ P_{2n} and $P_{2n}^{'}$ are arbitrary constants and $J_\beta(Nr)$, $J_\delta(Mr)$ and $Y_\delta(Nr)$, $Y_\beta(Mr)$ are the Bessel functions of first and second kind of order β and δ respectively.

Again, substituting Eqs.(33)-(35) in to Eqs.(30)-(31) and reducing to the simplest form as follows,

$$\varepsilon_{11}\left(E_n^{''}(r)+r^{-1}E_n^{'}(r)-c^2r^{-2}E_n(r)\right)+m_{11}\left(H_n^{''}(r)+r^{-1}H_n^{'}(r)-c^2r^{-2}H_n(r)\right)=0 \tag{40}$$

$$\varepsilon_{11}\left(H_n^{''}(r)+r^{-1}H_n^{'}(r)-c^2r^{-2}H_n(r)\right)+m_{11}\left(E_n^{''}(r)+r^{-1}E_n^{'}(r)-c^2r^{-2}E_n(r)\right)=0 \tag{41}$$

where $c^2=m^2+n^2$.

Solving Eq.(40) and Eq.(41),we can get,

$$E_n^{''}(r)+r^{-1}E_n^{'}(r)-c^2r^{-2}E_n(r)=0 \tag{42}$$

$$H_n^{''}(r)+r^{-1}H_n^{'}(r)-c^2r^{-2}H_n(r)=0 \tag{43}$$

The general solution of Eqs.(42) and (43) are as follows:

$$E_n(r,\theta,t)=\left(P_{3n}r^p+P_{3n}^{'}r^{-p}\right)\cos n\theta e^{i\omega t} \tag{44}$$

$$H_n(r,\theta,t)=\left(P_{4n}r^p+P_{4n}^{'}r^{-p}\right)\cos n\theta e^{i\omega t} \tag{45}$$

where P_{3n}, $P_{3n}^{'}$, P_{4n}, $P_{4n}^{'}$ are the arbitrary constants.

4 BOUNDARY CONDITIONS AND FREQUENCY EQUATIONS

Here, the problem of vibration of a magneto electro elastic polygonal plate is considered via hydrostatic stress and gravity. Since the boundary is irregular it is difficult to satisfy the boundary conditions directly. Hence, from the formulation of Nagaya [8], the Fourier expansion collocation method is applied to satisfy the boundary conditions. Thus the boundary conditions are obtained as,

$$\left(\Pi_{xx}\right)_j=\left(\Pi_{xy}\right)_j=\left(\mathbb{C}_r\right)_j=\left(\mathbb{N}_r\right)_j=0 \tag{46}$$

where x is the coordinate normal to the boundary and y is the tangential to the boundary Π_{xx} and Π_{xy} are the normal and shear stress. $(\ )_j$ is the value at the j^{th} segment of the cross section. Since the angle Γ_i between the

reference axis and normal to the j^{th} straight line boundary has a constant value in the segment as shown in the following figure

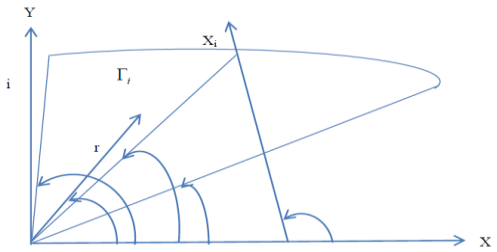

Fig.1
Line segment form.

In the above Fig.1 $1=\theta, 2=\theta_i, 3=(\theta_i+\theta_{i-1})/2, 4=\theta_{i-1}, 5=\Gamma_i$ .Transforming the vibration displacements into the Cartesian coordinates x_i and y_i the relation between the displacements for the *i-th* segment of straight line boundaries is

$$\begin{aligned} u_r &= u_r\cos(\theta-\gamma_i)-u_\theta\sin(\theta-\gamma_i), \\ u_\theta &= u_\theta\cos(\theta-\gamma_i)+u_r\sin(\theta-\gamma_i) \end{aligned} \tag{47}$$

and

$$\begin{aligned} \frac{\partial r}{\partial x_i} &= \cos(\theta-\gamma_i), \frac{\partial\theta}{\partial x_i} = -r^{-1}\sin(\theta-\gamma_i) \\ \frac{\partial r}{\partial y_i} &= \sin(\theta-\gamma_i), \frac{\partial\theta}{\partial y_i} = r^{-1}\cos(\theta-\gamma_i) \end{aligned} \tag{48}$$

Using the above Eqs. (47) and (48), the stress eqautions for the non homogeneity becomes,

$$\begin{aligned} \Pi_{xx} &= \left((\lambda+2\mu)\cos^2(\theta-\gamma_i)+\lambda\sin^2(\theta-\gamma_i)\right)u_{r,r}+r^{-1}\left((\lambda+2\mu)\sin^2(\theta-\gamma_i)+\lambda\cos^2(\theta-\gamma_i)\right)\left(u_r+u_{\theta,\theta}\right) \\ &+\frac{u_\theta}{2}\left(r^{-1}\left(u_\theta-u_{r,\theta}\right)-u_{\theta,r}\right)\sin 2(\theta-\gamma_i)=0 \\ \Pi_{xy} &= \mu\left(\left(u_{r,r}-r^{-1}u_{\theta,\theta}-r^{-1}u_r\right)\sin 2(\theta-\gamma_i)+\left(r^{-1}u_{r,\theta}+u_{\theta,r}-r^{-1}u_\theta\right)\cos 2(\theta-\gamma_i)\right)=0 \\ \mathrm{E}_x &= -\varepsilon_{11}E_{,r}-m_{11}H_{,r}=0 \\ \mathrm{M}_x &= -m_{11}E_{,r}-\mu_{11}H_{,r}=0 \end{aligned}$$

Applying the solution in the boundary condition (51) we arrive at the transformed form,

$$\begin{aligned} \left[\left(\mathrm{T}_{xx}\right)_j+\left(\overline{\mathrm{T}}_{xx}\right)_j\right]e^{i\omega t} &= 0 \\ \left[\left(\mathrm{T}_{xy}\right)_j+\left(\overline{\mathrm{T}}_{xy}\right)_j\right]e^{i\omega t} &= 0 \\ \left[\left(E_x\right)_j+\left(\overline{E}_x\right)_j\right]e^{i\omega t} &= 0 \\ \left[\left(M_x\right)_j+\left(\overline{M}_x\right)_j\right]e^{i\omega t} &= 0 \end{aligned} \tag{49}$$

where

$$
\begin{aligned}
\mathrm{T}_{xx} &= 0.5\left(P_{10}e_0{}^1 + P_{20}e_0{}^2 + P_{30}e_0{}^3\right) + \sum_{n=1}^{\infty}\left(P_{1n}e_n{}^1 + P_{2n}e_n{}^2 + P_{3n}e_n{}^3 + P_{4n}e_n{}^4\right)\\
\mathrm{T}_{xy} &= 0.5\left(P_{10}f_0{}^1 + P_{20}f_0{}^2 + P_{30}f_0{}^3\right) + \sum_{n=1}^{\infty}\left(P_{1n}f_n{}^1 + P_{2n}f_n{}^2 + P_{3n}f_n{}^3 + P_{4n}f_n{}^4\right)\\
\mathrm{E}_x &= 0.5\left(P_{10}g_0{}^1 + P_{20}g_0{}^2 + P_{30}g_0{}^3\right) + \sum_{n=1}^{\infty}\left(P_{1n}g_n{}^1 + P_{2n}g_n{}^2 + P_{3n}g_n{}^3 + P_{4n}g_n{}^4\right)\\
\mathrm{M}_x &= 0.5\left(P_{10}h_0{}^1 + P_{20}h_0{}^2 + P_{30}h_0{}^3\right) + \sum_{n=1}^{\infty}\left(P_{1n}h_n{}^1 + P_{2n}h_n{}^2 + P_{3n}h_n{}^3 + P_{4n}h_n{}^4\right)
\end{aligned}
\tag{50}
$$

For anti-symmetric mode

$$
\begin{aligned}
\overline{\mathrm{T}}_{xx} &= 0.5\left(\overline{P}_{40}\bar{e}_0{}^4\right) + \sum_{n=1}^{\infty}\left(\overline{A}_{1n}\bar{e}_n{}^1 + \overline{A}_{2n}\bar{e}_n{}^2 + \overline{A}_{3n}\bar{e}_n{}^3 + \overline{A}_{4n}\bar{e}_n{}^4\right)\\
\overline{\mathrm{T}}_{xy} &= 0.5\left(\overline{P}_{40}\bar{f}_0{}^4\right) + \sum_{n=1}^{\infty}\left(\overline{P}_{1n}\bar{f}_n{}^1 + \overline{P}_{2n}\bar{f}_n{}^2 + \overline{P}_{3n}\bar{f}_n{}^3 + \overline{P}_{3n}\bar{f}_n{}^3\right)\\
\overline{\mathrm{E}}_x &= 0.5\left(\overline{P}_{40}\bar{g}_0{}^4\right) + \sum_{n=1}^{\infty}\left(\overline{P}_{1n}\bar{g}_n{}^1 + \overline{P}_{2n}\bar{g}_n{}^2 + \overline{P}_{3n}\bar{g}_n{}^3 + \overline{P}_{4n}\bar{g}_n{}^4\right)\\
\overline{\mathrm{M}}_x &= 0.5\left(\overline{P}_{40}\bar{h}_0{}^4\right) + \sum_{n=1}^{\infty}\left(\overline{P}_{1n}\bar{h}_n{}^1 + \overline{P}_{2n}\bar{h}_n{}^2 + \overline{P}_{3n}\bar{h}_n{}^3 + \overline{P}_{4n}\bar{h}_n{}^4\right)
\end{aligned}
\tag{51}
$$

Using the Fourier series expansion to the boundary Eq. (46) along the boundary surfaces are expanded in the form of double Fourier series .The boundary conditions are obtained as, for symmetric mode,

$$
\begin{aligned}
&\sum_{m=0}^{\infty}\varepsilon_m\left[E_{m0}{}^1P_{10} + E_{m0}{}^2P_{20} + \sum_{n=1}^{\infty}\left(E_{mn}{}^1P_{1n} + E_{mn}{}^2P_{2n} + E_{mn}{}^3P_{3n}\right)\right]\cos m\theta = 0\\
&\sum_{m=0}^{\infty}\left[F_{m0}{}^1P_{10} + F_{m0}{}^2P_{20} + \sum_{n=1}^{\infty}\left(F_{mn}{}^1P_{1n} + F_{mn}{}^2P_{2n} + F_{mn}{}^3P_{3n}\right)\right]\sin m\theta = 0\\
&\sum_{m=0}^{\infty}\varepsilon_m\left[G_{m0}{}^1P_{10} + G_{m0}{}^2P_{20} + \sum_{n=1}^{\infty}\left(G_{mn}{}^1P_{1n} + G_{mn}{}^2P_{2n} + G_{mn}{}^3P_{3n}\right)\right]\cos m\theta = 0\\
&\sum_{m=0}^{\infty}\varepsilon_m\left[H_{m0}{}^1P_{10} + H_{m0}{}^2P_{20} + \sum_{n=1}^{\infty}\left(H_{mn}{}^1P_{1n} + H_{mn}{}^2P_{2n} + H_{mn}{}^3P_{3n}\right)\right]\cos m\theta = 0
\end{aligned}
$$

For anti-symmetric mode,

$$
\begin{aligned}
&\sum_{m=0}^{\infty}\left[\overline{E}_{m0}{}^3P_{30} + \sum_{n=1}^{\infty}\left(\overline{E}_{mn}{}^1P_{1n} + \overline{E}_{mn}{}^2P_{2n} + \overline{E}_{mn}{}^3P_{3n}\right)\right]\sin m\theta = 0\\
&\sum_{m=0}^{\infty}\varepsilon_m\left[\overline{F}_{m0}{}^3P_{30} + \sum_{n=1}^{\infty}\left(\overline{F}_{mn}{}^1P_{1n} + \overline{F}_{mn}{}^2P_{2n} + \overline{F}_{mn}{}^3P_{3n}\right)\right]\cos m\theta = 0\\
&\sum_{m=0}^{\infty}\left[\overline{G}_{m0}{}^3P_{30} + \sum_{n=1}^{\infty}\left(\overline{G}_{mn}{}^1P_{1n} + \overline{G}_{mn}{}^2P_{2n} + \overline{G}_{mn}{}^3P_{3n}\right)\right]\sin m\theta = 0\\
&\sum_{m=0}^{\infty}\left[\overline{H}_{m0}{}^3P_{30} + \sum_{n=1}^{\infty}\left(\overline{H}_{mn}{}^1P_{1n} + \overline{H}_{mn}{}^2P_{2n} + \overline{H}_{mn}{}^3P_{3n}\right)\right]\sin m\theta = 0
\end{aligned}
\tag{52}
$$

where

$$E_{mn}{}^{j}=\frac{2\varepsilon_n}{\pi}\sum_{\ell=1}^{S}\int_{\theta_{i-1}}^{\theta} e_n{}^{j}\left(R_\ell,\theta\right)\cos m\theta d\theta \qquad \overline{E}_{mn}{}^{j}=\frac{2\varepsilon_n}{\pi}\sum_{\ell=1}^{S}\int_{\theta_{i-1}}^{\theta} \overline{e}_n{}^{j}\left(R_\ell,\theta\right)\sin m\theta d\theta$$

$$F_{mn}{}^{j}=\frac{2\varepsilon_n}{\pi}\sum_{\ell=1}^{S}\int_{\theta_{i-1}}^{\theta} f_n{}^{j}\left(R_\ell,\theta\right)\sin m\theta d\theta \qquad \overline{F}_{mn}{}^{j}=\frac{2\varepsilon_n}{\pi}\sum_{\ell=1}^{S}\int_{\theta_{i-1}}^{\theta} \overline{f}_n{}^{j}\left(R_\ell,\theta\right)\cos m\theta d\theta$$

$$G_{mn}{}^{j}=\frac{2\varepsilon_n}{\pi}\sum_{\ell=1}^{S}\int_{\theta_{i-1}}^{\theta} g_n{}^{j}\left(R_\ell,\theta\right)\cos m\theta d\theta \qquad \overline{G}_{mn}{}^{j}=\frac{2\varepsilon_n}{\pi}\sum_{\ell=1}^{S}\int_{\theta_{i-1}}^{\theta} \overline{g}_n{}^{j}\left(R_\ell,\theta\right)\sin m\theta d\theta$$

$$H_{mn}{}^{j}=\frac{2\varepsilon_n}{\pi}\sum_{\ell=1}^{S}\int_{\theta_{i-1}}^{\theta} h_n{}^{j}\left(R_\ell,\theta\right)\cos m\theta d\theta \qquad \overline{H}_{mn}{}^{j}=\frac{2\varepsilon_n}{\pi}\sum_{\ell=1}^{S}\int_{\theta_{i-1}}^{\theta} \overline{h}_n{}^{j}\left(R_\ell,\theta\right)\sin m\theta d\theta$$

The coefficients $e_n{}^{i}\sim\overline{h}_n{}^{i}$ are given in the appendix.

5 NUMERICAL RESULTS AND DISCUSSIONS

To illustrate the analytical result presented earlier, now we consider the numerical example for which computational results are presented. The physical constants for the numerical computation is taken from copper at $42^{\circ}K$, Poisson ratio $\nu=0.3$, density $\rho=8.96\times10^{3}kg/m^{3}$, the Young's modulus $E=2.139\times10^{11}N/m^{2}$, $\lambda=8.20\times10^{11}kg/ms^{2}$, $\mu=4.20\times10^{10}kg/ms^{2}$, $c_v=9.1\times10^{-2}m^{2}/ks^{2}$ and $K=113\times10^{-2}kgm/ks^{2}$. The material properties of the magneto-electro elastic material based on Peng-Fei Hou et al.[40] are $\varepsilon_{11}=8.26\times10^{-11}C^{2}N^{-1}m^{-2}$, $\mu_{11}=-5\times10^{-6}Ns^{2}/C^{2}$, $m_{11}=-3612\times10^{-11}Ns/VC$. The geometric relations for the polygonal cross-sections given by Nagaya [8] as $R_i/a=\left[\cos\left(\theta-\gamma_i\right)\right]^{-1}$, $R_i/b=\left[\cos\left(\theta-\gamma_i\right)\right]^{-1}$, $\gamma_i=\gamma_i$. To study the convergence and validation of the present study, the frequency equation of a thick polygonal cross-sectional plate without non homogeneous parameter and other interacting field variables is chosen to show the exactness of the result obtained in the present case with the results of Nagaya [2]. The non-dimensional frequencies $|\Omega|$, obtained for a ring shaped polygonal plates using Fourier expansion collocation method, with clamped edges, in both the Author and Nagaya's [2], have exact coincidence, which is shown in Table 1.

Table 1

Comparative display of non-dimensional frequencies $|\Omega|$ of polygonal plate of Author results with the results of Nagaya [8] of a ring shaped polygonal plates with clamped (ICOC) edges.

a/b	Mode	Triangle		Square		Pentagon		Hexagon	
		Nagaya[8]	Author	Nagaya[8]	Author	Nagaya[8]	Author	Nagaya[8]	Author
0.1	n_1	4.148	4.146	4.850	4.849	4.995	4.995	5.061	5.061
	n_2	4.392	4.393	4.997	4.997	5.132	5.132	5.163	5.162
	n_3	4.547	4.551	5.889	5.886	5.627	5.626	5.784	5.783
0.15	n_1	4.269	4.267	5.128	5.127	5.297	5.296	5.367	5.365
	n_2	4.510	4.511	5.271	5.272	5.419	5.418	5.449	5.446
	n_3	4.769	4.765	6.069	6.068	5.782	5.784	5.951	5.945
0.2	n_1	4.413	4.412	5.431	5.431	5.636	5.636	5.712	5.712
	n_2	4.622	4.613	5.573	5.572	5.742	5.741	5.771	5.772
	n_3	4.924	4.924	6.315	6.316	5.995	5.996	6.180	6.181
0.25	n_1	4.474	4.573	5.757	5.756	6.018	6.017	6.103	6.103
	n_2	4.739	4.738	5.910	5.911	6.106	6.104	6.138	6.136
	n_3	5.019	5.016	6.627	6.627	6.264	6.265	6.470	6.471

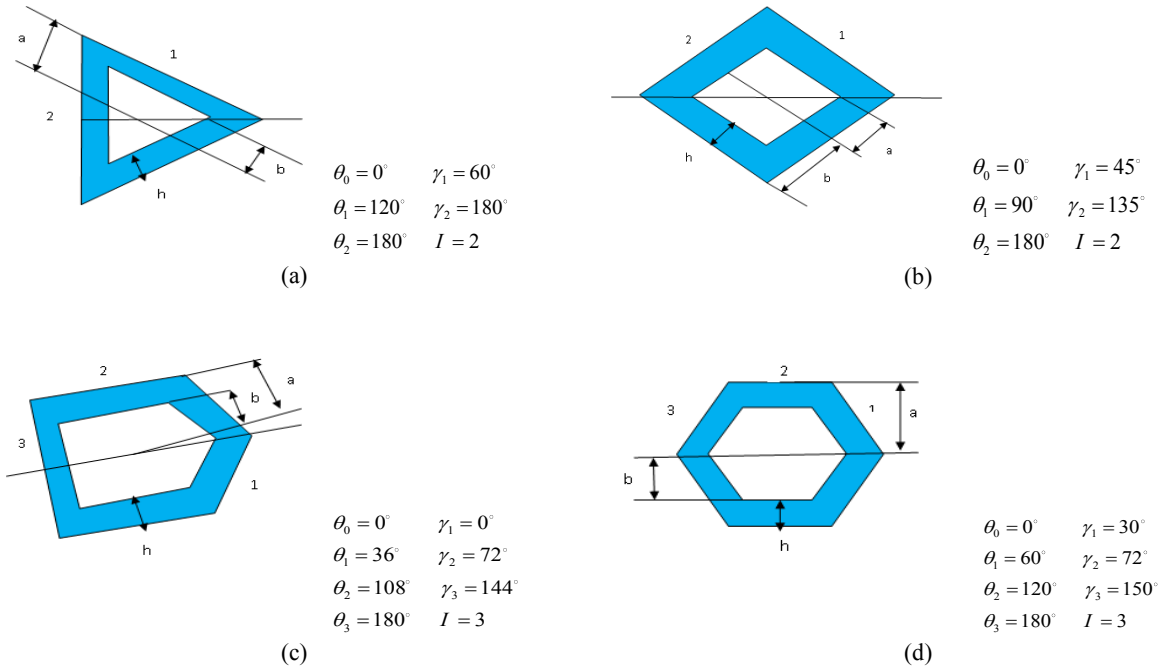

Fig.2
Geometry of Polygonal shapes of plate (a. Triangular, b. Square, c. Pentagon, d. Hexagon).

A graph is drawn for the variation of radial stress Π_{rr} with plate radius r for IFOC and IFOF edge boundary conditions via $g = 0.0, 9.8$ for the polygonal plate in Fig.3 and Fig.4. From the Figs. 3 and 4, it is observed that, the radial stress Π_{rr} increases with respect to its radius r, also it is noted that the radial stress attains the maximum value in IFOF edge boundary than the radial stress of IFOC edge boundary conditions and also in higher gravity. The energy level is higher in hexagonal and pentagonal cross sections as compared to other cross sections. Figs. 5- 6 display the distribution of displacement u against the radius r with IFOC and IFOF of polygonal plates for $g = 0.0, 9.8$. From the Figs. 5 and 6, it is observed that the displacement is higher for a plate with inner free and outer free edges. It is shown that, the displacement of the pentagon and hexagon cross section is higher in both the values of the gravity.

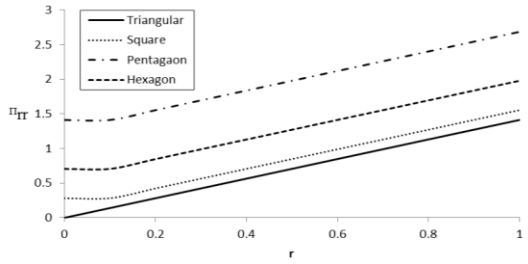

Fig.3
Radial stress with radius of the polygonal plate with IFOC edges via $g = 0.0$.

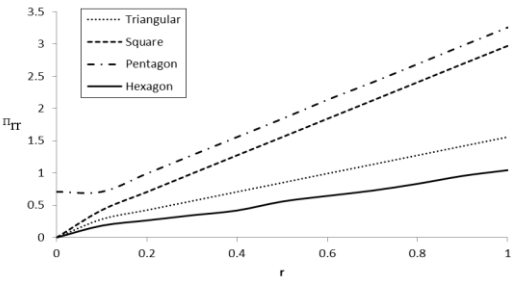

Fig.4
Radial stress with radius of the polygonal plate with IFOF edges via $g = 9.8$.

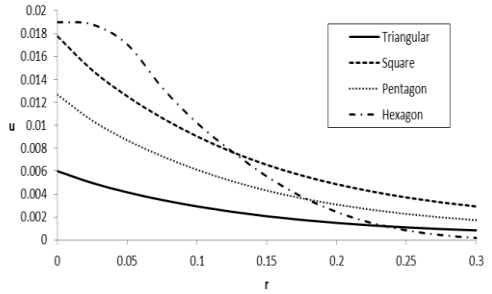

Fig.5
Displacement with radius of the polygonal plate with IFOC edges via $g = 0.0$.

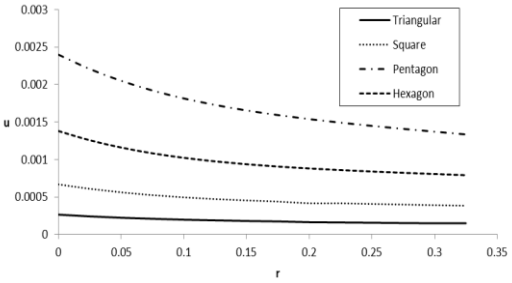

Fig.6
Displacement with radius of the polygonal plate with IFOF edges via $g = 9.8$.

Dispersion curves are plotted for the variation of electric displacement $\mathbb{C}_r$ with radius r of Triangle, Square, Pentagon and Hexagonal cross-sectional plates with IFOC and ICOF edges via $g = 0.0, 9.8$ in Figs. 7-8. From the Figs. 7 and 8, it is observed that the dispersions behavior of Triangle, Pentagon and Square, Hexagon are similar to each other at $g = 0.0, 9.8$. The crosses over points denote the transfer of energy between the modes of vibrations due to the hydrostatic stress, gravity and clamped- free boundaries. Figs. 9-10 show magnetic displacement $\mathbb{N}_r$ with radius r of polygonal plates with IFOC and IFOF boundary conditions via $g = 0.0, 9.8$. The magnetic displacement is higher in the lower values of radius and became linear in the other part of radius in both boundary conditions and higher in the case of $g = 9.8$ and ICOF edge. It is shown that, the magnetic displacement of the pentagon and hexagon plate is more in two cases due to the symmetry of cross section and the influence of other interactive fields.

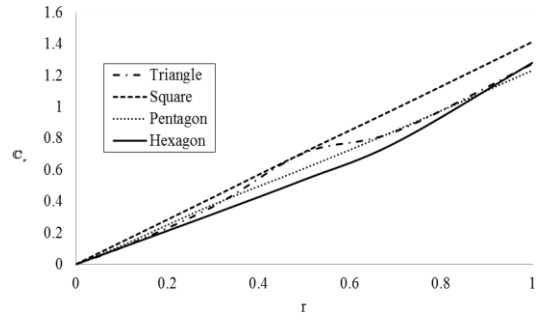

Fig.7
Dispersion of electric potential with radius of polygonal plate with IFOC edges via $g = 0.0$.

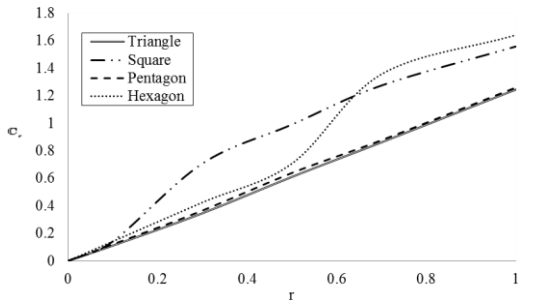

Fig.8
Dispersion of electric potential with plate radius of polygonal plate with and ICOF edges via $g = 9.8$.

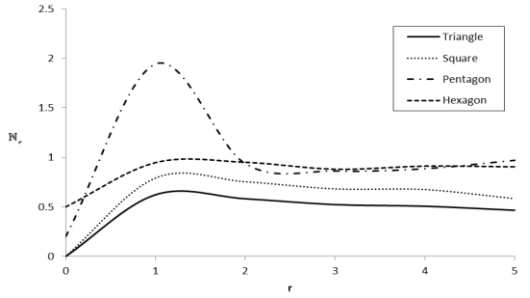

Fig.9
Dispersion of magnetic potential with plate radius of polygonal plate with IFOC edges via $g = 0.0$.

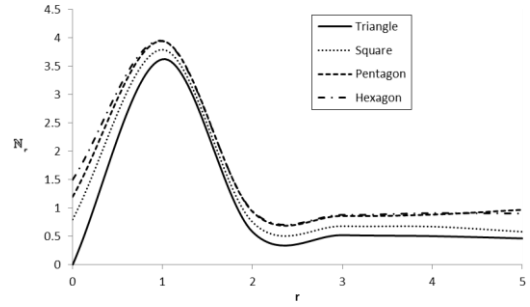

Fig.10
Dispersion of magnetic potential with plate radius of polygonal plate with ICOF edges via $g = 9.8$.

Figs.11-14 illustrates the frequency distribution $|\Omega|$ with radius r of Triangle, Square, Pentagon and Hexagonal cross-sectional plates with different boundary conditions and aspect ratio through $g = 9.8$. From the Figs. 11-14, it is noted that the frequency increases as the radius increases in all the boundary conditions.

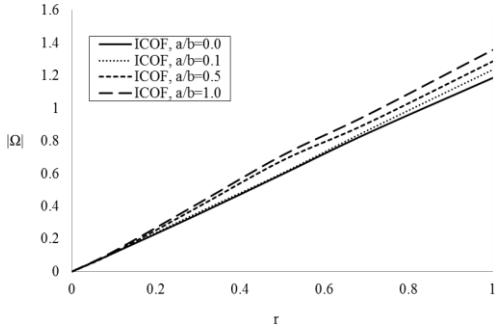

Fig.11
Frequency with radius of triangular cross-sectional plate with ICOF edges via $g = 9.8$.

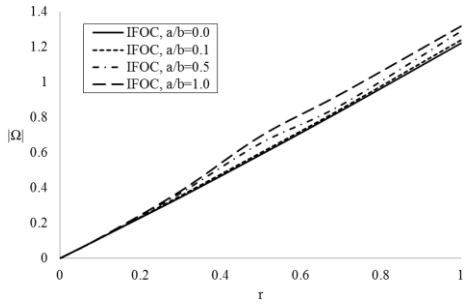

Fig.12
Frequency with radius of square cross-sectional plate with IFOC edges via $g = 9.8$.

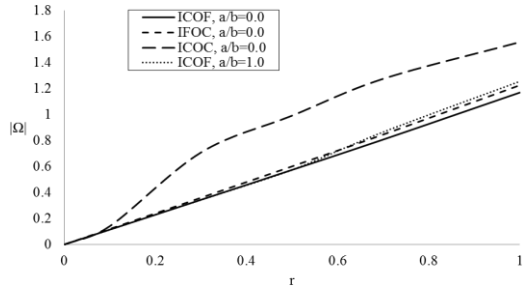

Fig.13
Frequency with radius of pentagonal cross-sectional plate with IFOC, ICOF edges via $g = 9.8$.

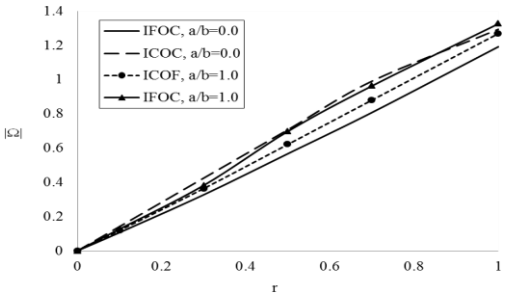

Fig.14
Frequency with radius of hexagonal cross-sectional plate with IFOC, ICOF edges via $g = 9.8$.

6 CONCLUSIONS

The clamped free non homogeneous wave propagation on a magneto electro elastic plate of polygonal shape is studied in this paper. The interactive force terms gravity and the hydro static stress on the polygonal plate also have been derived using linear elasticity theory. Fourier expansion collocation method is used to solve the irregular boundary of the polygonal shape of the plate. The numerical result of the stress, mechanical, displacement, electric displacement, magnetic displacement and non-dimensional frequency of the wave in the various shapes such as triangle, square, pentagon and hexagon cross section plates with IFOC, ICOC, ICOF edges and fixed gravity are computed and the graphical representations are presented. We concluded that

- The hydrostatic stress, gravity and non-homogeneity of the poly plate have important role on the distribution of physical variables.
- The boundary edge IFOC and IFOF are noted to be more significant in all the field variables.
- Pentagon and Hexagon cross section plate attain higher values in all the physical quantities.
- The Fourier expansion collocation method gave faster convergence in irregular boundaries.
- This type of study is more important in the construction of foundation of footing, turbine disks, floor and roof with irregular boundaries.

APPENDIX

$$e_n^{\,1} = 2\{\,\beta(\beta-1)J_\beta(Nr)+(Nr)J_{\beta+1}(Nr)\,\}\cos 2(\theta-\gamma_i)\cos n\theta$$
$$-r^2\{\,N^2(\bar{\lambda}+2\cos^2(\theta-\gamma_i)\,\}J_n(Nr)\cos n\theta$$
$$\bar{e}_n^{\,1} = 2\{\,\beta(\beta-1)J_\beta(Nr)+(Nr)J_{\beta+1}(Nr)\,\}\sin 2(\theta-\gamma_i)\sin n\theta$$
$$-r^2\{\,N^2(\bar{\lambda}+2\cos^2(\theta-\gamma_i)\,\}J_\beta(N)\sin n\theta$$
$$e_n^{\,2} = \left\{\,n(\delta-1)J_\delta(Mr)-(Mr)J_\delta(Mr)\,\right\}\cos 2(\theta-\gamma_i)\cos n\theta$$
$$-\left\{\left(\delta(\delta+2)\right)+n^2-(Mr)^2\right)\frac{J_\delta(Mr)}{2}-(Mr)J_{\delta+1}(Mr)\right\}\sin n\theta\sin 2(\theta-\gamma_i)$$

$$\overline{e_n^{\,2}} = \left\{ \; n(\delta-1)J_\delta(Mr) - (Mr)J_\delta(Mr) \; \right\} \sin 2(\theta-\gamma_i) \sin n\theta$$

$$-\left\{ \left(\delta(\delta+2)\right) + n^2 - (Mr)^2 \right) \frac{J_\delta(Mr)}{2} - (Mr)J_{\delta+1}(Mr) \right\} \cos n\theta \cos 2(\theta-\gamma_i)$$

$$e_n^3 = 0, e_n^4 = 0$$

$$f_n^{\,1} = \left[2\left\{ \beta J_\beta(Nr) - (Nr)J_{\beta+1}(Nr) \right\} + \left((Nr)^2 - \beta^2 - n^2 \right) J_\beta(Nr) \right] \cos n\theta \sin 2(\theta-\gamma_i)$$

$$+2n\left\{ \; (\beta-1)J_\beta(Nr) - (Nr)J_{\beta+1}(Nr) \; \right\} \sin n\theta \cos 2(\theta-\gamma_i).$$

$$\overline{f_n^{\,1}} = \left[2\left\{ \beta J_\beta(Nr) - (Nr)J_{\beta+1}(Nr) \right\} + \left((Nr)^2 - \beta^2 - n^2 \right) J_\beta(Nr) \right] \sin \theta \cos 2(\theta-\gamma_i)$$

$$+2n\left\{ \; (\beta-1)J_\beta(Nr) - (Nr)J_{\beta+1}(Nr) \; \right\} \cos n\theta \sin 2(\theta-\gamma_i).$$

$$f_n^{\,2} = 2n\left[\delta J_\delta(Mr) - (Mr)J_{\delta+1}(Mr) \right] \cos n\theta \sin 2(\theta-\gamma_i) +$$

$$2\left\{ \; \left[\delta J_\delta(Mr) - (Mr)J_{\delta+1}(Mr) \right] + \left[(Mr)^2 - \delta^2 - n^2 \right] J_\delta(Mr) \; \right\} \sin n\theta \cos 2(\theta-\gamma_i)$$

$$\overline{f_n^{\,2}} = 2n\left[\delta J_\delta(Mr) - (Mr)J_{\delta+1}(Mr) \right] \sin n\theta \cos 2(\theta-\gamma_i) +$$

$$2\left\{ \; \left[\delta J_\delta(Mr) - (Mr)J_{\delta+1}(Mr) \right] + \left[(Mr)^2 - \delta^2 - n^2 \right] J_\delta(Mr) \; \right\} \cos n\theta \sin 2(\theta-\gamma_i)$$

$$f_n^3 = 0, f_n^4 = 0$$

REFERENCES

[1] Akbarzadeh A.H., Pasini D., 2014, Multiphysics of multilayered functionally graded cylinders under prescribed hygrothermoagnetoelectro-mechanical loading, *Journal of Applied Mechanics* **81**: 041018-1-13.

[2] Arefi M., Koohi Faegh R., Loghman A., 2016, The effect of axially variable thermal and mechanical loads on the 2D thermoelastic response of FG cylindrical shell, *Journal of Thermal Stresses* **39**: 1539-1559.

[3] Khoshgoftar M., Rahimi G.H., Arefi M., 2013, Exact solution of functionally graded thick cylinder with finite length under longitudinally non-uniform pressure, *Mechanics Research Communications* **51**: 61-66.

[4] Arefi M,, Rahimi G.H., 2012, The effect of non homogeneity and end supports on the thermo elastic behaviour of a clamped –clamped FG cylinder under mechanical and thermal loads, *International Journal of Pressure Vessels and Piping* **96**: 30-37.

[5] Arefi M., 2013, Nonlinear thermoelastic analysis of thick-walled functionally graded piezoelectric cylinder, *Acta Mechanicca* **11**: 2771-2783.

[6] Loghman A., Nasr M., Arefi M., 2017, Nonsymmetric thermo mechanical analysis of a functionally graded cylinder subjected to mechanical, thermal and magnetic loads, *Journal of Thermal Stresses* **40**: 765-782.

[7] Rahimi G.H., 2011, Application and analysis of functionally graded piezoelectrical rotating cylinder as mechanical sensor subjected to pressure and thermal loads, *Applied Mathematics and Mechanics* **32**: 997-1008.

[8] Nagaya K., 1981, Dispersion of elastic waves in bars with polygonal cross section, *Journal of Acoustical Society of America* **70**: 763-770.

[9] Hutchinson J.R., 1979, Axisymmetric flexural vibrations of a thick free circular plate, *Journal of Applied Mechanics* **46**: 139-144.

[10] Arefi M., Allam M.N.M., 2015, Nonlinear responses of an arbitrary FGP circular plate resting on the Winkler-Pasternak foundation, *Smart Structures and Systems* **16**: 81-100.

[11] Nagaya K., 1980, Method for solving vibration problems of a plate with arbitrary shape, *The Journal of the Acoustical Society of America* **67**: 2029-2033.

[12] Arefi M., 2015, Nonlinear electromechanical analysis of a functionally graded square plate integrated with smart layers resting on Winkler-Pasternak foundation, *Smart Structures and Systems* **16**: 195-211.

[13] Chakraverty S., Jindal R., Agarwal V.K., 2005, Flexural vibrations of non-homogeneous elliptic plates, *Indian Journal of Engineering and Materials Sciences* **12**: 521-528.

[14] Tanigawa Y., 1995, Some basic thermoelastic problems for nonhomogeneous structural materials, *Applied Mechanics Reviews* **48**: 287-300.

[15] Annibale F.D., 2014, Linear stability of piezoelectric controlled discrete mechanical system under non constructive positional forces, *Meccanica* **50**: 1-15.

[16] Selvamani R., 2015, Wave propagation in a rotating disc of polygonal cross section immersed in an inviscid fluid, *Cogent Engineering* **2**(1): 1-20.
[17] Bin W., Jiangong J., Cunfu H., 2008, Wave propagation in non-homogeneous magneto-electro-elastic plates, *Journal of Sound and Vibrations* **317**: 250-264.
[18] Chen W.Q., Lee K.Y., Ding H.J., 2005, On free vibration of non-homogeneous transversely isotropic magneto-electro-elastic plate, *Journal of Sound and Vibration* **279**: 237-251.
[19] Li J.Y., 2000, Magneto electro elastic multi-inclusion and inhomogeneity problems and their applications in composite materials, *International Journal of Engineering Science* **38**: 1993-2011.
[20] Kong T., Li D.X., Wang X., 2009, Thermo-magneto-dynamic stresses and perturbation of magnetic field vector in non-homgeneous hollow cylinder, *Applied of Mathematical Modelling* **33**: 2939-2950.
[21] Kumar R., Sharma P., 2016, Variational principle, uniqueness and reciprocity theorems in porous magneto thermo elastic medium, *Cogent Mathematics* **3**(1): 1-25.
[22] Pan E., 2001, Exact solution for simply supported and multilayered magneto-electro-elastic plates,transactions of the ASME, *Journal of Applied Mechanics* **68**: 608-618.
[23] Pan E., Heyliger P.R., 2002, Free vibration of simply supported and multilayered magneto-electro-elastic plates, *Journal of Sound and Vibrations* **252**: 429-442.
[24] Pan E., Han F., 2005, Exact solution for functionally graded and layered magneto-electro-elastic plates, *International Journal of Engineering and Sciences* **43**: 321-339.
[25] Feng W.J., Pan E., 2008, Dynamic fracture behavior of an internal interfacial crack between two dissimilar magneto-electro-elastic plates, *Engineering Fracture Mechanics* **75**: 1468-1487.
[26] Kumar R., 1998, Wave propagation in a generalized thermo microstretch elastic solid, *International Journal of Engineering Sciences* **36**: 891-912.
[27] Selim M., 2007, Waves propagation in an initially stressed dissipative cylinder, *Applied Mathematical Sciences* **1**: 1419-1427.
[28] Kumar R., 2011, Wave propagation in transversely isotropic generalized thermo elastic half space with voids under initial stress, *Multidiscipline Modelling in Materials and Structures* **7**: 440-468.
[29] Akbarov S.D., 2011, Tortional wave dissipation in a finitely pre-strained hollow sandwich circular cylinder, *Journal of Sound and Vibration* **330**: 4519-4537.
[30] Kakar R., 2013, Magneto elastic torsional surface waves in prestressed fiber reinforced medium, *International Journal of Mathematical Mechanics* **9**: 1-19.
[31] Kakar R., 2013, Wave propagation in compressed materials with reinforcement in preferred direction subjected to gravity and initial compression, *Journal of Chemical Biological and Physicsl Sciences* **3**(2):1468-1481.
[32] Kumari N., 2015, Edge waves in initially stressed visco elastic plate, *Journal of Physics: Conference Series-International Conference of Vibration Problems* **662**: 012011.
[33] De S.N., 1974, Influence of gravity on wave propagation in an elastic cylinder, *Journal of Acoustical Society of America* **55**: 919-921.
[34] Dey S., 1992, Tortional wave propagation in an initially stressed cylinder, *Proceedings of the Indian National Science Academy* **58**: 425-429.
[35] Chen W.Q., 2012, Waves in pre stretched incompressible soft electro active cylinders: Exact Solution, *Acta Mechanica* **25**: 530-541.
[36] Wilson A.J., 1977, Wave propagation in thin pre-stressed elastic plates, *International Journal of Engineering Science* **15**: 245-251.
[37] Zhang X.M., YU J.G., 2013, Effects of initial stresses on guided waves in unidirectional plates, *Archives of Mechanics* **65**: 3-26.
[38] Lotfy K.H., 2019, Magneto rotation fibre-reinforced thermoelastic gravity and energy dissipation, *International Journal for Computational Methods in Engineering Science and Mechanics* **1550**: 2287-2295.
[39] Ahmed S.H., 1999, Influence of gravity on the propagation of waves in granular medium, *Applied Mathematics and Computation* **101**: 269-280.
[40] Hou P.F., Andrew Y.T., Leung Ding H.J., 2008, Point heat source on the surface of a semi-infinite transversely isotropic electro-magneto-thermo-elastic material, *International Journal of Engineering Sciences* **46**: 273-285.
[41] Chen J., Chen H., Pan E., 2006, Free vibration of functionally graded,magneto-thermo-electro-elastic and multilayered plates, *Act Mechanica Solida Sinica* **19**: 60-66.